MOLECULAR AND CELLULAR BIOLOGY, Jan. 2003, p. 665–676 Vol. 23, No. 2
0270-7306/03/$08.00+0 DOI: 10.1128/MCB.23.2.665–676.2003

Susceptibility of Lysosomes to Rupture Is a Determinant for Plasma Membrane Disruption in Tumor Necrosis Factor Alpha-Induced Cell Death

Koh Ono, Sung O. Kim, and Jiahuai Han*

Department of Immunology, The Scripps Research Institute, La Jolla, California 92037

Received 15 August 2002/Returned for modification 18 September 2002/Accepted 22 October 2002

Since a release of intracellular contents can induce local inflammatory responses, mechanisms that lead to loss of plasma membrane integrity in cell death are important to know. We showed previously that deficiency of the plasma membrane Ca^{2+} ATPase 4 (PMCA4) in L929 cells impaired tumor necrosis factor alpha (TNF-α)-induced enlargement of lysosomes and reduced cell death. The lysosomal changes can be determined by measuring the total volume of intracellular acidic compartments per cell (VAC), and we show here that inhibition of the increase in VAC due to PMCA4 deficiency not only reduced cell death but also converted TNF-α-induced cell death from a process involving disruption of the plasma membrane to a cell demise with a nearly intact plasma membrane. The importance of the size of lysosomes in determining plasma membrane integrity during cell death was supported by the observations that chemical inhibitors that reduce VAC also reduced the plasma membrane disruption induced by TNF-α in wild-type L929 cells, while increases in VAC due to genetic mutation, senescence, cell culture conditions, and chemical inhibitors all changed the morphology of cell death from one with an originally nearly intact plasma membrane to one with membrane disruption in a number of different cells. Moreover, the ATP depletion-mediated change from apoptosis to necrosis is also associated with the increases of VAC. The increase in lysosomal size may due to intracellular self-digestion of dying cells. Big lysosomes are easy to rupture, and the release of hydrolytic enzymes from ruptured lysosomes can cause plasma membrane disruption.

Cell death can take place in morphologically distinct apoptotic and necrotic processes (29). Apoptotic cells are defined by fragmented nuclei with condensed chromatin and shrunken cytoplasm within a nearly intact plasma membrane. Because the intracellular contents of dead cells are not released into surrounding tissues, apoptosis is a safe way to eliminate unwanted individual cells in metazoans (29). Necrosis, in contrast, is not accompanied by organized DNA degradation and is characterized by cytoplasmic swelling and plasma membrane breakage. Disruption of the plasma membrane leads to a release of intracellular materials, which are toxic to other cells and which can cause inflammation (29).

In vitro studies have shown that a trigger such as tumor necrosis factor alpha (TNF-α) can induce apoptosis in one cell type but necrosis in others (3, 15, 53). TNF-α-induced necrosis and apoptosis share some common signaling events downstream of the TNF-α receptor such as the recruitment of TRADD, FADD, and other cytosolic effector proteins to the cytosolic domains of TNF-α receptors (15, 33, 54). Cellular events such as mitochondrial permeability transition and free-radical generation have been implicated in TNF-α-induced apoptosis and necrosis (16, 20, 23). Death-modulating molecules such as Bcl-2 family members and metaxin can influence TNF-α-induced necrosis and apoptosis (26, 50, 57). Apoptosis and necrosis also appear to be controlled by parallel pathways (21). It is known that, in many apoptotic cell deaths where cell clearance by phagocytosis is lacking, secondary necrosis ensues (29). In some systems apoptosis can be effectively inhibited by caspase inhibitors, but the cell still undergoes a necrosis-like cell death (9, 10, 20, 21, 28, 37, 42). TNF-α-induced death of L929 cells was even enhanced by inhibition of caspase (55). Apoptosis and necrosis can be interconvertible under certain conditions. ATP depletion can convert cell death from an apoptotic morphology to a necrotic morphology (11, 31), suggesting that intracellular ATP levels regulate the mode of cell death. This notion was further supported by the fact that overactivation of poly(ADP-ribose) polymerase, a well-known substrate of caspases, leads to the depletion of the substrate β-NAD, resulting in a reduction of ATP level and subsequent necrotic cell death (18, 19, 36).

Because of the important role of necrosis in causing inflammation, we are interested in finding cellular events that cause necrotic cell death in response to physiological stimuli. TNF-α-induced L929 cell death produced necrotic phenotypes such as cytoplasmic swelling and plasma membrane disruption (3, 15, 53). We used genetic mutations to study TNF-α-induced necrosis in L929 cells (41, 56, 57). Deficiency of plasma membrane calcium ATPase 4 (PMCA4) was found to provide resistance to TNF-α-induced necrosis in L929 cells (41). Lysosomal trafficking was altered in this mutant line ($PMCA^{mut}$), as lysosome exocytosis was increased after TNF-α treatment (41). We have demonstrated that the resistance to death in $PMCA^{mut}$ cells was mediated by preventing the TNF-α-induced increase of the total volume of acidic compartments (VAC; constituted mostly by lysosomes) (41), consistent with a number of previous reports that lysosomes are involved in cell death (5, 8, 25, 32, 39, 40). Here we show that, in addition to

* Corresponding author. Mailing address: Department of Immunology IMM-32, The Scripps Research Institute, 10550 North Torrey Pines Rd., La Jolla, CA 92037. Phone: (858) 784-8704. Fax: (858) 784-8665. E-mail: jhan@scripps.edu.

the reduction of TNF-α-induced cell death in PMCA4-deficient cells, the dead PMCA^{mut} cells shrank within a nearly intact plasma membrane, which is an apoptotic characteristic. The inhibition of plasma membrane disruption in these cells is mediated by a reduction in VAC, which resulted from a reduction in lysosome size (41). The role of the VAC in controlling plasma membrane integrity was further supported by the increase in the VAC caused by genetic mutation, senescence, or cultural conditions, all of which lead to a loss of plasma membrane integrity in normally apoptotic processes. Moreover, an increase of the VAC is also required for ATP depletion-mediated switching from apoptosis to necrosis. Since disintegration of lysosomes occurred prior to plasma membrane disruption in cell deaths (41, 59), VAC, which reflects the size of lysosomes, may be linked to lysosomal disruption. Lysosomal enlargement occurring in a death program should alter the membrane tension of lysosomes and therefore increase their susceptibility to rupture. Here, we showed that larger lysosomes were much easier to disrupt. The size of lysosomes is a risk factor for the instability of lysosomes, which is a determinant for plasma membrane integrity or disruption during cell death.

MATERIALS AND METHODS

Materials. Murine TNF-α was provided by Vladimir Kravchenko of The Scripps Research Institute. Human TNF-α was obtained from R&D Systems (Minneapolis, Minn.). Fas monoclonal antibody (MAb) CH11 was obtained from Medical and Biological Laboratories (Nagoya, Japan). LysoTracker green and LysoTracker blue were obtained from Molecular Probes (Eugene, Oreg.). Acridine orange and other chemicals were from Sigma (St. Louis, Mo.) unless otherwise indicated below.

Cell culture. All cell lines were obtained from the American Type Culture Collection (Manassas, Va.) and were cultured under the recommended conditions. PMCA4-deficient L929 cells were described in our previous paper (41). Primary fibroblasts were prepared as follows. Skin samples were washed with phosphate-buffered saline (PBS) and then incubated with 0.05% trypsin-EDTA for 60 min at 37°C. Dermal samples were then cut into small (2-mm) squares and plated in six-well plates. Sterile 22-mm-diameter glass coverslips were placed over the specimens, and Dulbecco's modified Eagle medium was added. The medium was changed every 3 to 4 days. L929 (murine fibrosarcoma) cells, MCF-7 (human adenocarcinoma) cells, and Jurkat (human T-cell leukemia) cells were maintained in RPMI 1640 containing 10% fetal bovine serum, 2 mM glutamate, 100 U of penicillin/ml, and 100 μg of streptomycin/ml.

ATP depletion. ATP depletion was achieved by incubating cells in the presence of 10 μM oligomycin (Sigma) in glucose-free RPMI 1640 (Gibco BRL, Rockville, Md.) containing 2 mM pyruvate and 10% dialyzed fetal bovine serum. Under these conditions, oligomycin inhibits mitochondrial F_0F_1-ATPases and the depletion of glucose halts glycolysis so that no ATP-producing machinery operates. Intracellular ATP levels were measured by using the ATP bioluminescence assay kit HS II (Roche Molecular Biochemicals) in accordance with the manufacturer's protocol.

Transient transfection of Jurkat cells. Electroporation was used to transfect Jurkat cells. Cells (2×10^7/ml) were electroporated with 10 μg of DNA at 960 μF and 300 V. Approximately 50% of the cells were killed by electroporation. To remove the dead cells, the cells were resuspended in RPMI 1640 after electroporation. Five milliliters of Ficoll-Paque solution was layered under the cell suspension in 50-ml tubes. The tubes were centrifuged for 30 min in a Sorvall H-1000B rotor at 2,000 rpm ($800 \times g$) at room temperature. Live cells that floated on the top of the high-density solution were collected and washed twice with RPMI medium.

Measurement of VAC. Cells in various stages were harvested and then incubated at 37°C for 15 min with 100 ng of LysoTracker (Molecular Probes, Inc.)/ml. Cells were then washed, pelleted, and resuspended in 1 ml of PBS for measurement of fluorescence derived from the aggregated LysoTracker in acidic compartments. The healthy cells (with intact lysosomes) were gated, and the mean value of the fluorescence intensity was used as the relative value of VAC.

Cell viability assay using PI staining plus FSC. The integrity of the plasma membrane was assessed by determining the ability of cells to exclude propidium iodide (PI; Sigma). Cells were trypsinized, collected by centrifugation, washed once with PBS, and resuspended in PBS containing 1 μg of PI/ml. The levels of PI incorporation were quantified by flow cytometry on a FACScan flow cytometer. Cell size was evaluated by forward-angle light scattering (FSC). PI-negative cells with normal size were considered to be live cells.

Blue light irradiation. The cells were loaded with acridine orange (5 μg/ml) for 15 min at 37°C and then kept for another 15 min in RPMI medium without phenol red for another 15 min before being exposed to blue light for different periods of times. The light was emitted from a 200-W mercury arc lamp (Osram, Berlin, Germany). A BG 38 blue light-transmitting filter (allowing passage of 450- to 500-nm light) and a heat-absorbing filter were placed in the beam path. The intensity of red fluorescence was measured by fluorescence-activated cell sorter 2 h after blue light exposure. The cell viability was measured for 4 h after blue light exposure.

DNA ladder assay. Cells were lysed in lysis buffer (10 mM Tris-HCl [pH 8.0], 100 mM NaCl, 0.5% sodium dodecyl sulfate, 25 mM EDTA, 0.1 mg of protease K/ml) and incubated at 50°C overnight. DNA was extracted with phenol-chloroform, precipitated by adding NaCl to 0.3 M and 2 volumes of ethanol, and centrifuged for 15 min at $16,000 \times g$. The DNA pellets were resuspended in TE (Tris-HCl [pH 7.8], 1 mM EDTA) buffer with 0.1 mg of RNase I/ml for 1 h at room temperature and then treated with 0.1 mg of protease K/ml overnight at 37°C. DNA was further extracted with phenol-chloroform and precipitated as described above and resuspended in 20 μl of TE buffer. Equal amounts of DNA were separated on 2% agarose gel and stained with ethidium bromide for visualization.

RESULTS

PMCA4 deficiency switches the mode of TNF-α-induced cell death in L929 cells from plasma membrane disruption to a nearly intact plasma membrane. TNF-α-induced L929 cell death shows necrotic features: a disrupted plasma membrane and cell swelling (Fig. 1A, parental L929) (55). Interestingly, we found that there was less cell death in PMCA4-deficient (PMCA^{mut}) L929 cells after TNF-α treatment (41) and the dead cells had shrunk (Fig. 1A, PMCA^{mut}). Genomic DNA analyzed before and after TNF-α treatment demonstrated that TNF-α produced DNA fragmentation in PMCA^{mut} cells although a large amount of DNA was required to view the fragmentation on an agarose gel (Fig. 1A, right). Since DNA fragmentation in a certain subline of L929 cells can be observed after TNF-α treatment (12, 22, 52) but did not precede cell death (12), we speculated that the machinery for DNA fragmentation is present in our L929 cell line. But this process may be slow and unpronounced and may therefore be masked by the predominant pathway that leads to cell death with necrotic morphology. When the major death pathway in PMCA^{mut} cells was impaired, DNA fragmentation became apparent. Thus, unlike the death of parental L929 cells, the death of PMCA^{mut} cells induced by TNF-α had some characteristics similar to apoptosis.

PI exclusion is a widely used method to determine the integrity of a plasma membrane. The dead cells produced by TNF-α treatment of L929 cells showed high levels of PI stain, indicating the disruption of the plasma membrane. We gated these dead cells as group R1 and gated the healthy cells as group R3 (Fig. 1B, parental L929). As we reported previously (41), PMCA4 deficiency increased the survival rate of L929 cells that were treated with TNF-α (55 versus 7.6%; Fig. 1B). Consistent with Fig. 1A, the majority of dead cells in the PMCA^{mut} line were smaller (R2 group) based on flow cytometry analysis using FSC. Moreover, these dead cells had less PI stains than wild-type cells, indicating that plasma membrane

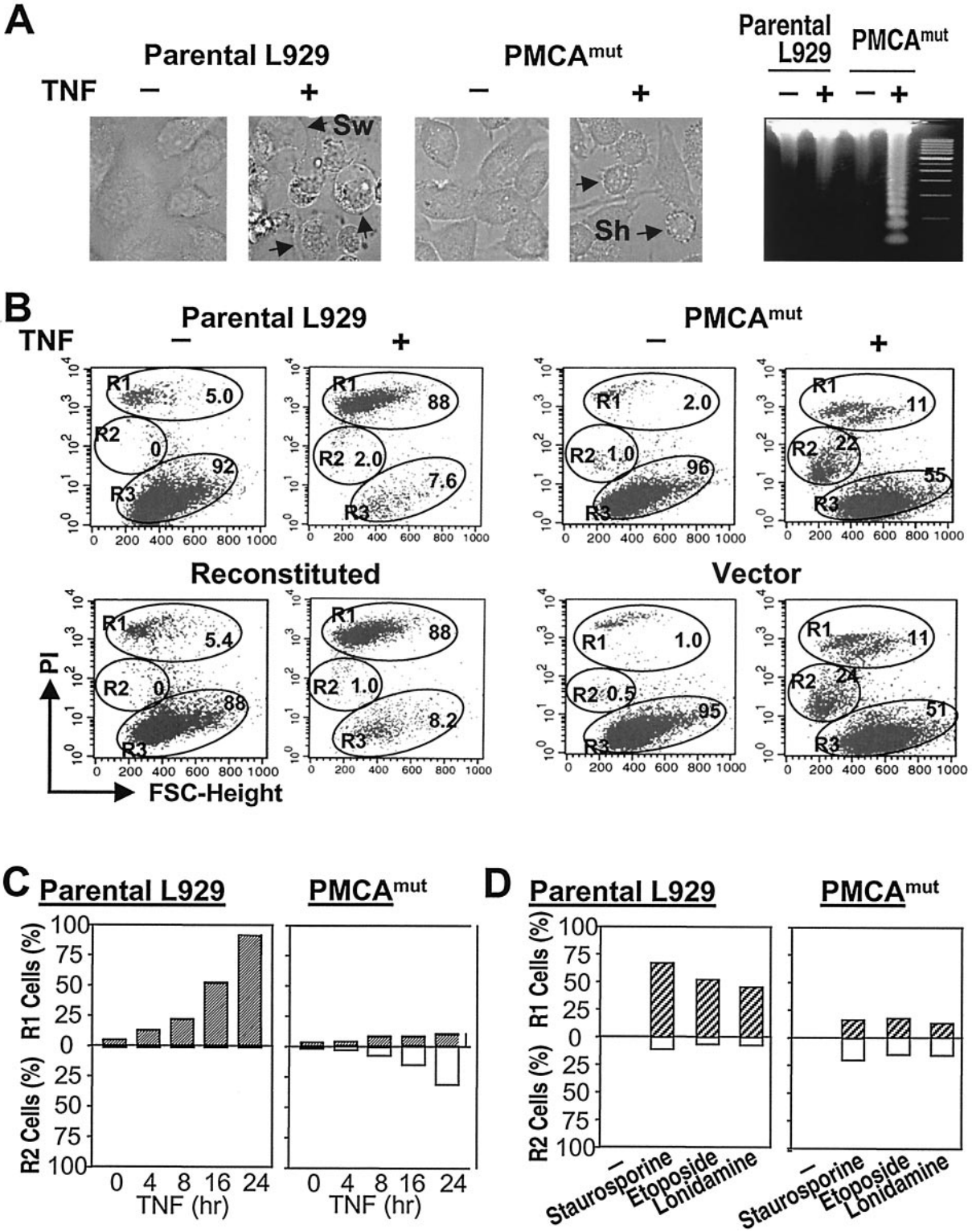

FIG. 1. PMCA4 deficiency changes the morphology of TNF-α-induced cell death in L929 cells. (A) Parental and PMCA^{mut} L929 cells were untreated (−) or treated with 100 ng of TNF-α/ml (+) for 10 h. Cells were analyzed by microscopy. The genomic DNA was isolated and electrophoresed on a 2% agarose gel. Parental cells died with swelling (Sw), while PMCA^{mut} cells were shrunken (Sh). DNA laddering was detected in TNF-α-treated PMCA^{mut} cells but not in parental cells. (B) Parental, PMCA^{mut}, PMCA4-reconstituted, and empty vector-transfected PMCA^{mut} cells were untreated (−) or treated with TNF-α (+) for 10 h, and the cells were analyzed by PI exclusion plus FSC. The samples were analyzed by flow cytometry (FACSan flow cytometer [Becton Dickinson]) with CellQuest acquisition and analysis software. Different populations of dead and live cells were gated as R1, R2, and R3. R1 cells, necrotic cells that lost plasma membrane integrity, as indicated by PI-positive stains; R2 cells, apoptotic cells that had reduced size and low level of PI stains; R3 cells, healthy cells of normal size with PI-negative stains. The percentages of these three groups of cells are marked. (C) Parental and PMCA^{mut} cells were treated with TNF-α for various times and analyzed as described for panel B. The percentages of R1 and R2 cells are shown. (D) Parental and PMCA^{mut} cells were treated with staurosporine (1 μM), etoposide (10 μM), or lonidamine (10 μM) for 24, 24, and 4 h, respectively, and analyzed as described for panel B. The percentages of R1 and R2 cells are shown.

integrity was better maintained (Fig. 1B, PMCA^{mut}). This phenotype change was caused by a PMCA4 mutation because the reconstitution of PMCA4 expression in PMCA^{mut} cells switched the phenotype of dead cells to that of R1 (Fig. 1B, reconstituted). In contrast, transfection of an empty vector into PMCA^{mut} cells had no effect on the phenotype associated with cell death (Fig. 1B, vector). Overexpression of PMCA4 in wild-type L929 cells did not affect TNF-α-induced cell death (data not shown). We have shown previously that PMCA4 mutation-mediated TNF-α resistance is due to the inhibition of the TNF-α-induced increase in VAC (41). Since the reduction of the TNF-α-induced increase in the VAC in PMCA^{mut} cells correlated with the switch of the phenotype of cell death, it is possible that acidic compartments (constituted mostly by lysosomes) play a role in controlling the mode of cell death.

The different intensities of PI stains in R1 and R2 cells indicated a difference in plasma membrane integrity of the dead cells. However, complete loss of plasma membrane integrity (R1) could just be a late status of R2 cells. To determine whether R2 group cells are an intermediate between healthy cells (R3 group) and R1 group cells, we measured the percentages of these different groups of cells in parental and PMCA^{mut} L929 cells treated with TNF-α for various times. There were no R2 group cells throughout the course of TNF-α treatment in parental cells (Fig. 1C, left). The presence of R1 and R2 group cells in TNF-α-treated PMCA^{mut} cells was not time dependent (Fig. 1C, right). These data suggest that the generation of R2 cells is not due to a slower cell death process in PMCA^{mut} cells and that R2 cells are not the precursors of R1 cells. Thus, R1 and R2 cells were generated by different modes of cell death. The effect of PMCA4 mutation on the cell death induced by staurosporine, etoposide, and lonidamine is similar to its effect on the cell death induced by TNF-α (Fig. 1D).

R1 (disrupted plasma membrane) and R2 (nearly intact plasma membrane) types of cell death in different cell death systems. To ensure that the R1 and R2 types of dead cells can be generally used to distinguish different modes of cell death, we examined the R1 and R2 groups of cells in three different cell death systems. Fas ligation-induced Jurkat cell death is a prototypic model system used in apoptosis studies. Jurkat cells treated with 0.1 μg of the agonistic anti-human Fas MAb CH11/ml for various times showed shrunken cytoplasm and the formation of apoptotic bodies under the microscope (Fig. 2A, top). Most of the dead cells were small with low levels of PI stain and therefore can be gated as R2 group cells (Fig. 2A, bottom). TNF-α-induced cell death of MCF-7, which has also frequently been used in studies of apoptosis, produces both shrunken and swollen phenotypes (Fig. 2B, top). The dead MCF-7 cells are composed of both R1 and R2 groups of cells (Fig. 2B, bottom). TNF-α-induced cell death in L929 cells was associated with cell swelling (Fig. 2C, top). Almost all of the dead cells lost their plasma membrane integrity and belonged to group R1 (Fig. 2C, bottom). R1 and R2 gating of dead cells can distinguish different types of cell death in different systems (Jurkat and L929 cells) and can also discriminate two types of dead cells produced in the same system (MCF-7 cells). Thus, R1 and R2 cells can be used to study the mode of cell death.

The VAC is linked to plasma membrane disruption. We showed previously that TNF-α-treated PMCA^{mut} cells had a smaller VAC than wild-type L929 cells (41) and that TNF-α-induced dead cells in PMCA^{mut} cells were mainly the R2 type, while parental wild-type cells were all of the R1 type (Fig. 1). These data suggest that a large VAC could be linked to plasma membrane disruption in wild-type L929 cells. A direct way to test this possibility is to increase the VAC by other means in PMCA^{mut} or other cells whose death was associated with a nearly intact plasma membrane. Indigestible solute sucrose can cause lysosome fusion, which results in an increase of the VAC (7, 24, 51). The large VAC in sucrose-treated cells can be used to examine whether a large VAC can cause plasma membrane disruption, i.e., switch the R2 type cell death to the R1 type cell death. Culturing parental wild-type L929, PMCA^{mut} L929, MCF-7, and Jurkat cells in the presence of 30 mM sucrose resulted in a significant increase in the VAC, as measured by staining with LysoTracker, an acidotropic probe used to stain lysosomes and other types of acidic compartments; in contrast, 30 mM glucose did not have such an effect (Fig. 3, left). The cells were healthy and proliferated at the same rate in sucrose- and glucose-containing media (data not shown). We precultured cells in these two culture mediums for 12 h to permit an increase of the VAC in sucrose-treated cells and then treated L929 and MCF-7 cells with TNF-α and treated Jurkat cells with the Fas antibody. The increase of the VAC due to sucrose in PMCA^{mut} cells reduced R2 type cell death and increased the percentage of R1 group cells (Fig. 3A, right). Since all parental L929 cells died as R1 group cells, sucrose treatment did not have an effect on the phenotype associated with cell death (Fig. 3B). MCF-7 cells died with mixed R1 and R2 phenotypes (Fig. 2B and 3C). Culturing in a sucrose-containing medium significantly increased the percentage of R1 group cells (Fig. 3C, right). Fas ligation-induced Jurkat cells died mostly with an R2 phenotype, and many cells died with an R1 phenotype when the cells were pretreated with sucrose (Fig. 3D, right). Since the PMCA4 mutation led to a reduction of the TNF-α-induced increase of the VAC and reduced the plasma membrane disruption and since an increase of the VAC in PMCA^{mut}, MCF-7, and Jurkat cells led to plasma membrane disruption, the VAC appears to be linked to plasma membrane disruption.

To further evaluate the notion that the VAC is linked to plasma membrane disruption in necrotic cell death, we examined the mode of cell death in the cells that had a naturally occurring large VAC. Murine *beige*, homologue of the gene of the human autosomal recessive disorder Chediak-Higashi syndrome, is associated with the formation of giant lysosomes (2, 38, 43). It has been shown that the fibroblasts isolated from *beige* (Lyst^{bg}) mice have bigger lysosomes than wild-type mice with the same background (43). Primary fibroblasts from *beige* and control (C57BL/6) mice were prepared and stained with LysoTracker. VAC was approximately two- to threefold larger in *beige* fibroblasts than in control fibroblasts, confirming that *beige* fibroblasts have large lysosomes (Fig. 4A, left). As expected, death stimulus TNF-α plus cycloheximide (CHX) increased VAC in both wild-type and mutant fibroblasts. Because of the high basal level of VAC in *beige* fibroblasts, the absolute value of VAC in TNF-α–CHX-treated *beige* fibroblasts was much higher than that in control cells (Fig. 4A, left). We also observed that almost all *beige* fibroblasts died as R1 group cells, whereas at least 50% of dead cells in control fibroblasts fell into the R2 group (Fig. 4A, right).

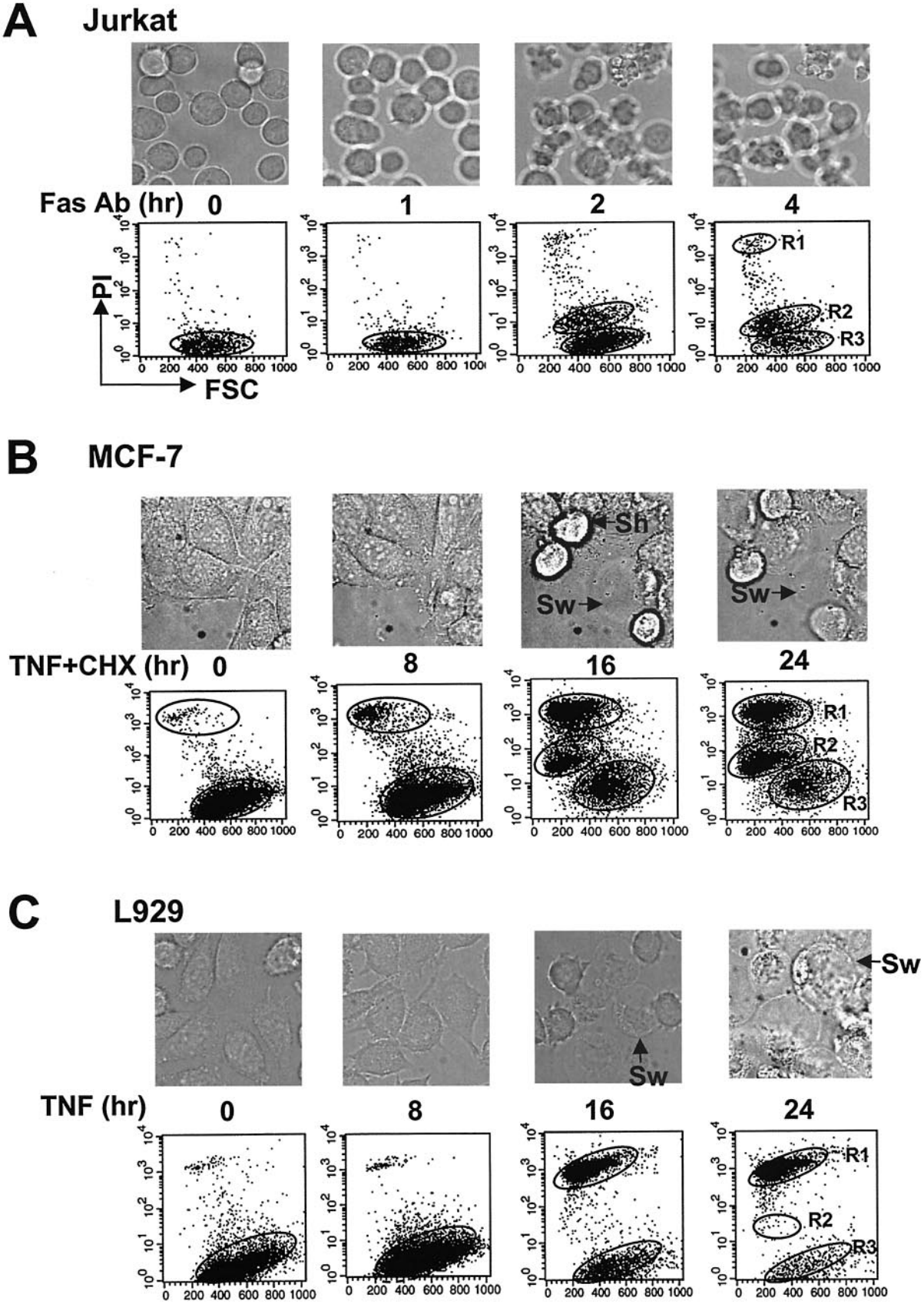

FIG. 2. R1 and R2 types of cell death in different cell death systems. (A) Jurkat cells were treated with the Fas MAb (Fas Ab; 0.5 μg/ml) for various time periods. (B) MCF-7 cells were treated with TNF-α and CHX (5 μg/ml) for various time periods. (C) L929 cells were treated with TNF-α for various time periods. The cells were analyzed by microscopy and by PI exclusion plus FSC as described for Fig. 1. Sh and Sw are as defined for Fig. 1.

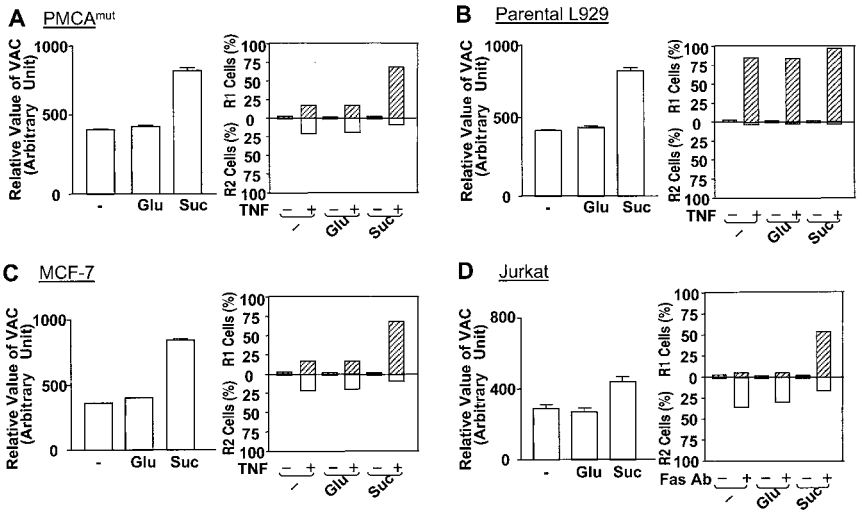

FIG. 3. Increases of the VAC due to sucrose can lead to the loss of plasma membrane integrity in cell death. PMCA^{mut} L929 cells (A), parental L929 cells (B), MCF-7 cells (C), and Jurkat cells (D) were untreated (−) or treated with 30 mM glucose (Glu) or 30 mM sucrose (Suc). The relative value of the VAC was determined by LysoTracker staining. The L929 cells and MCF-7 cells were treated with TNF-α or TNF-α plus CHX, respectively, for 10 h. The Jurkat cells were treated with the Fas MAb for 3 h. The results are means ± standard errors (n = 3 to 6). The cells were then analyzed by PI exclusion plus FSC as described for Fig. 1. The percentages of R1 and R2 cells are shown.

It is known that the total volume of lysosomes increases during replicative aging (30). We analyzed the VAC in primary fibroblasts of C57 mice after different passages in culture. As shown Fig. 4B, left, an increase in VAC with the number of passages was detected by LysoTracker staining. Treatment with TNF-α plus CHX produced more R1 group cells in aged cells than in younger cells (Fig. 4B, right), which again supports the idea that the VAC is linked to plasma membrane disruption.

BAX is a proapoptotic member of the Bcl-2 family protein. Overexpression of BAX led to apoptosis. Caspase inhibitor zVAD can prevent BAX-induced DNA degradation, but the cells died with cytoplasmic vacuolation (58). We transiently expressed BAX in Jurkat cells and treated these cells with or without zVAD. Expression of BAX led to slight increases in VAC, but the presence of zVAD greatly enhanced the VAC in the cells (Fig. 4C, left). zVAD's effect required BAX expression because zVAD treatment alone did not have an effect on the VAC. The dead cells induced by BAX were predominantly R2 type cells, and zVAD treatment of the BAX-expressed cells caused a significant increase in the number of R1 cells (Fig. 4C, right). These data again support the notion that the VAC is linked to the mode of cell death.

ATP depletion-mediated conversion of apoptosis to necrosis is associated with the increase of VAC. It is well known that ATP depletion can switch the cell death mode from apoptosis to necrosis (11, 31). ATP depletion was shown to block caspase-3 activation and other downstream apoptosis signaling, but how necrosis was turned on by ATP depletion was unknown (11, 31). If the VAC is an essential determinant for the breakdown of the plasma membrane in cells undergoing the death process, then the VAC should be increased in the ATP depletion-mediated switch of apoptosis to necrosis. To determine whether the VAC plays a role in ATP depletion-mediated conversion of apoptosis to necrosis, we examined whether ATP depletion had an effect on the VAC. Jurkat cells were maintained in a glucose-free medium supplemented with pyruvate to allow only mitochondrial ATP production. The cells were healthy and underwent apoptosis after Fas ligation (data not shown) (11, 31). ATP depletion was achieved by treating the cells with oligomycin, a blocker of mitochondrial ATP synthesis. We stained acidic compartments with LysoTracker in cells with or without the predepletion of ATP. Fas ligation led to an increase in the LysoTracker stain, and a much stronger stain was observed in ATP-depleted cells than in the cells without ATP depletion (Fig. 5A). As reported by others (11, 31), Fas ligation induced shrinkage of Jurkat cells (apoptosis) and ATP depletion changed the morphology of dying cells to cytoplasmic swelling (necrosis) (Fig. 5A, phase). In parallel experiments, we measured the VAC using flow cytometry. Fas ligation led to a substantial increase of the VAC in ATP-depleted cells, while only a small increase was observed in the Jurkat cells that had not been preemptied with ATP (Fig. 5B). The VAC was slightly increased in the first hour of oligomycin treatment alone, and the VAC reduced to background at later time points (Fig. 5B), indicating that the ATP depletion alone did not have much of an effect on VAC. As reported by others (11, 31), ATP depletion dramatically increased necrotic (R1 group) cells and eliminated apoptotic (R2 group) cells (Fig. 5C). Thus, ATP depletion-mediated increases of the VAC in Fas-ligated cells are correlated with ATP depletion-mediated conversion of the modes of cell death.

TNF-α–CHX-treated MCF-7 cells were examined under conditions with or without the depletion of ATP. Similar to what was found for Jurkat cells, ATP depletion significantly enhanced the TNF-α-induced increase of the VAC (Fig. 5D) and switched TNF-α-induced cell death from the R2 group to the R1 group (Fig. 5E). These data again suggest the notion that the increase of the VAC causes a switch in the death

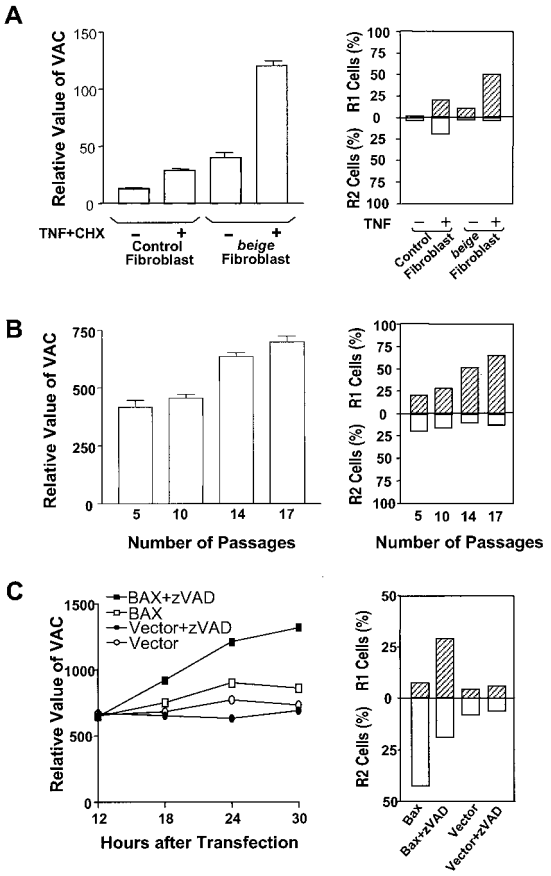

FIG. 4. The loss of plasma membrane integrity is associated with a large VAC in cells. Fibroblasts of *beige* mice (Lyst^{bg}) or control mice (C57BL/6) (A) and C57BL/6 fibroblasts of different passages (B) were treated with or without TNF-α plus CHX for 10 h. Half of each sample was analyzed by LysoTracker staining, and the other half was analyzed by PI exclusion plus FSC. The relative value of the VAC was determined by the intensity of LysoTracker staining. The results represent means ± standard errors ($n = 3$). The percentages of R1 and R2 cells are shown. (C) Jurkat cells were cotransfected with the BAX expression vector or an empty vector and a green fluorescent protein (GFP) expression vector. The cells were left untreated or treated with zVAD (50 μM) for 12 h after transfection. GFP expression was used to identify transfected cells by using a fluorescence-activated cell sorter. The relative value of the VAC in transfected cells was measured by staining the cells with LysoTracker at 12, 18, 24, and 30 h after transfection. The viability of cells was analyzed 30 h after transfection by PI exclusion plus FSC. Percentages of R1 and R2 are shown.

mode. A direct way to demonstrate the role of the VAC in switching the mode of cell death is to inhibit the switching process by preventing the increase of the VAC. Although there is no highly specific and effective method available at present, forskolin, an adenylate cyclase activator, is capable, via stimulating lysosomal exocytosis, of reducing the VAC in some cells, including MCF-7 cells (41, 46). To inhibit the increase of the VAC caused by ATP depletion in TNF-α-treated MCF-7 cells, we included forskolin in the course of our experiments. Forskolin did not have much influence on TNF-α–CHX-induced cell death under normal cell culture conditions, indicating that this molecule does not interfere with cell death pathways used by TNF-α in MCF-7 cells (Fig. 5F, left). Forskolin did not affect intracellular ATP levels (Fig. 5F, right). Forskolin inhibited the increase in the VAC (41, 46) and prevented the switch from the R2 phenotype to the R1 phenotype under ATP-depleted conditions (Fig. 5F, left), suggesting that an increase of the VAC is required for the conversion between the two modes of cell death in ATP-depleted cells.

Reagents that influence lysosomal exocytosis modulate the mode of cell death. We have previously shown that promoting lysosomal exocytosis inhibits the increase of the VAC induced by death stimuli and that blocking lysosomal exocytosis enhances the increase of the VAC (41). Due to the linkage between the VAC and plasma membrane disruption in cell death, we next examined whether the agents that had an influence on lysosomal exocytosis affect the mode of cell death. An increase in intracellular calcium concentration was found to be a trigger of lysosomal exocytosis in some cells including L929 and MCF-7 cells (41, 47), and agents that elevate cytosolic cyclic AMP also potentiate exocytosis in these two cell lines (41, 46). Actin microfilament-stabilizing agent jasplakinolide, tubulin-depolymerizing agent nocodazole, and adenylyl cyclase inhibitor MDL 12,330A are structurally unrelated compounds that are known to inhibit lysosomal exocytosis (1, 46). These lysosomal exocytosis stimuli or inhibitors were known to have effects other than those on lysosome exocytosis. Because their cellular targets were different and because all had effects on lysosome exocytosis, we think their effect on the VAC warrants investigation. We have determined that the incubation of these reagents with L929 and MCF-7 did not cause detectable cell death in 48 h (data not shown). We treated L929 cells with calcium ionophore A-23187 or adenylate cyclase activator forskolin to reduce the VAC during TNF-α treatment. As shown in Fig. 6A the TNF-α-induced increase of the VAC was inhibited (left) and the mode of cell death was switched from R1 to R2 (right), supporting the idea that reducing the VAC helps in the maintenance of plasma membrane integrity. As expected, treatment with nocodazole, jasplakinolide, or MDL-12330A, which inhibits lysosomal exocytosis, did not have much effect on the VAC in TNF-α-treated L929 cells and the cell death mode was still R1 (Fig. 6A). Promoting lysosomal exocytosis in MCF-7 cells reduced the increase of VAC and decreased R1 cells in TNF-α-treated cells (Fig. 6B). Blocking lysosomal exocytosis enhanced the increase of VAC in MCF-7 cells and switched R2 cells to the R1 group (Fig. 6B). These data are consistent with the notion that a large VAC tends to cause plasma membrane disruption.

Large lysosomes are more susceptible to disruption. It is known that the leakage of lysosomes, the major component of acidic compartments, can cause plasma membrane disruption (necrosis) depending on the level of lysosome leakage (4). Since the surface tension is related to the size of the lysosome, the larger lysosomes should be easier to break down. In addition, the larger lysosomes should be more difficult to repair than smaller lysosomes when damage occurs. Disruption of large lysosomes can cause more-severe damage to cells than that of smaller lysosomes because more lysosomal contents are released. Thus, the VAC could be a key risk factor for plasma membrane disruption. Here we perform experiments to confirm that larger lysosomes are easier to disrupt.

Acridine orange is a lysosometrophic weak base, a metachromatic fluorochrome, and a photosensitizer as well. Acri-

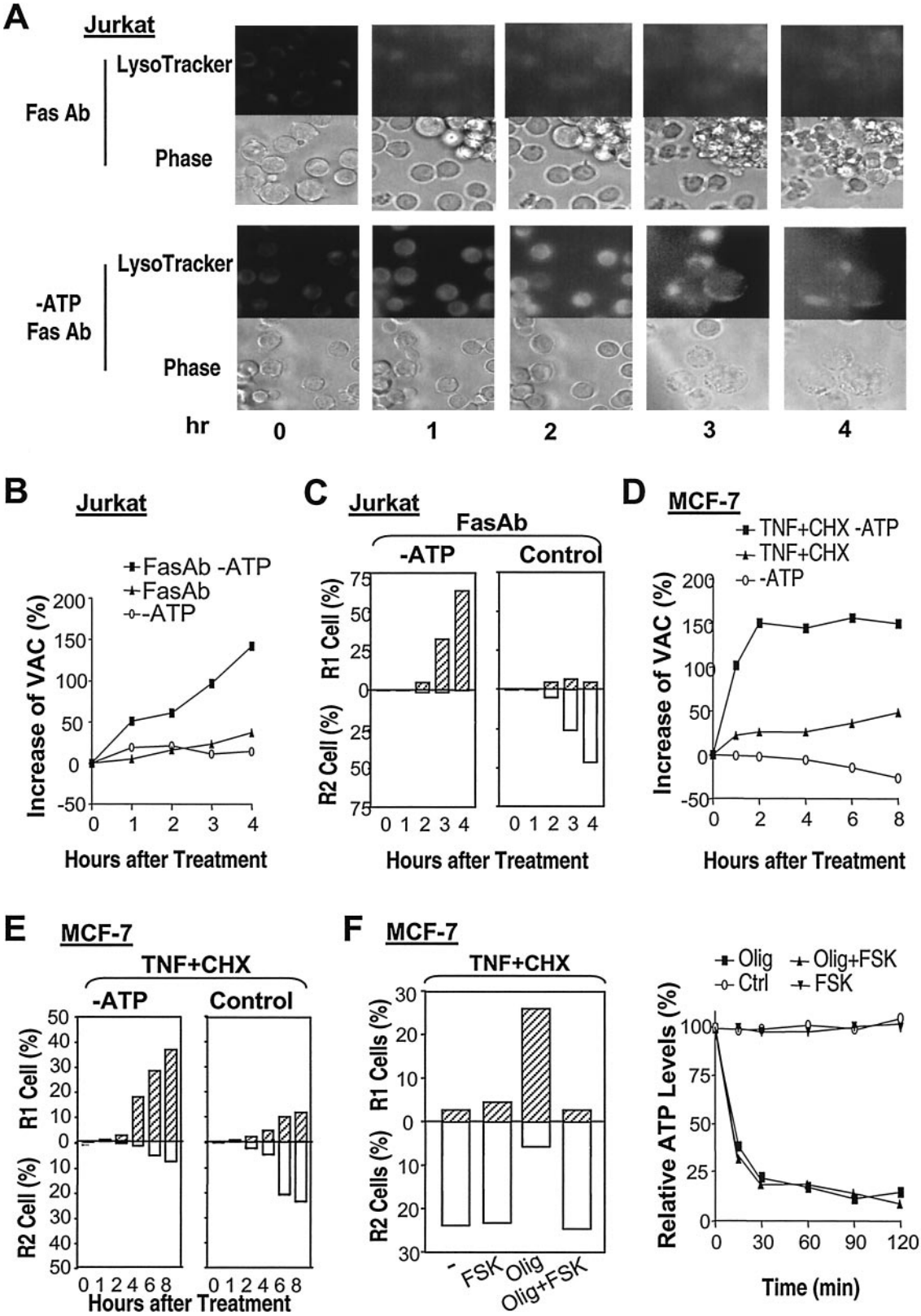

FIG. 5. ATP depletion-mediated conversion of apoptosis to necrosis is associated with an increase of VAC. (A) Jurkat cells with or without the depletion of ATP were treated with the Fas MAb for different periods of time, stained with LysoTracker, and analyzed by microscopy. (B) Jurkat cells with or without depletion of ATP were treated with or without the Fas MAb. Relative values of the VAC were determined at different time points after Fas MAb addition. The percent increases of the VAC are shown. (C) Jurkat cells were treated as described for panel B and analyzed by PI exclusion plus FSC. The percentages of R1 and R2 cells are shown. (D) MCF-7 cells with or without the depletion of ATP were treated with

dine orange selectively accumulates in cellular acidic vacuolar compartments. The leakage of acridine orange from the acidic compartments to the cytosol shifts the fluorescence from red to green (4). Because acridine orange is a photosensitizer, irradiation of acridine orange-loaded cells with intense blue light leads to photo-oxidation of lysosomal membranes and may subsequently disrupt the lysosomes (4). To evaluate whether large lysosomes are more easily broken down than small lysosomes, we examined whether there were any differences between large and small lysosomes in their sensitivities to blue light-induced lysosome disruption. MCF-7 cells were cultured for 12 h in a medium containing either sucrose, which promotes the formation of enlarged lysosomes (Fig. 3), or glucose, which does not affect the formation of lysosomes. These cells were loaded with acridine orange for 30 min and then treated with blue light of 10×10^4 lx for 0, 0.5, 1, 2, or 5 min. There was a higher percent reduction of red fluorescence in sucrose-treated MCF-7 cells than in glucose-treated MCF-7 cells (Fig. 7A), thus indicating that more lysosome disruption occurs in the cells with larger lysosomes. We also examined lysosome leakage in primary fibroblasts that had large lysosomes (from *beige* mice) and normal lysosomes (from C57BL/6 mice). As shown in Fig. 7B, the red fluorescence was decreased more in fibroblasts from *beige* mice than in the fibroblasts from C57BL/6 mice. Thus, large lysosomes are more susceptible to disruption.

It was reported that minor photo-oxidation of the lysosomal membrane can be repaired and does not cause cell death, that moderate damage of the lysosomal membrane (partial lysosomal leakiness) leads to apoptosis, and that severe photo-oxidation results in necrosis (4). Here we compared modes of cell death resulting from the disruption of normal and large lysosomes. When the same level of photo-oxidation was applied, the cells with large lysosomes had more cell deaths and produced more R1 cells (Fig. 7C and D). These data support the idea that large lysosomes are more susceptible to rupture and that their damage is more difficult to repair.

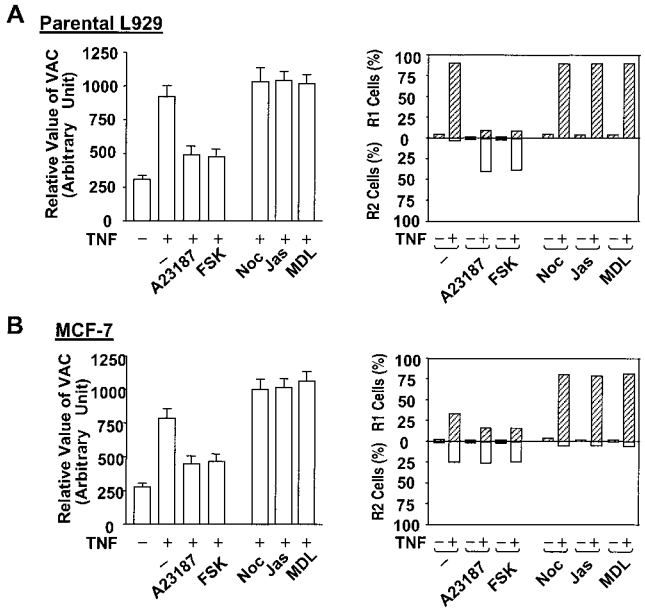

FIG. 6. Inhibition of TNF-α-induced increases in the VAC increases the percentage of R2 cells, and enhancement of TNF-α-induced VAC increases the percentage of R1 cells. Parental L929 cells (A) and MCF-7 cells (B) were untreated or treated with TNF-α or TNF-α plus CHX in the presence or absence of A-23187 (1 μM), forskolin (FSK), nocodazole (Noc; 10 μM), jasplakinolide (Jas; 0.3 μM), or MDL-12330A (MDL; 50 μM) for 10 h. The VAC (left) and percentages of R1 and R2 cells (right) were measured.

DISCUSSION

Alteration in the mode of cell death can affect the pathophysiology of a disease. For instance, conversion of an apoptotic cell death to necrosis can contribute to pathological processes because of uncontrolled release of cellular contents, causing local inflammation as well as the elicitation of unwanted autoimmune responses. The data presented in this study indicate that lysosomes play a key role in determining whether the integrity of the plasma membrane can be maintained or lost during cell death. The VAC, determined mostly by the size of lysosomes, is correlated with the degree of plasma membrane disruption. An increase of the VAC due to either intrinsic or extrinsic factors of a cell can change the cell death modes from apoptotic to necrotic (disruption of plasma membrane). Inhibition of death stimulus-induced increases of the VAC can reduce plasma membrane disruption. The properties of big lysosomes such as being highly susceptible to rupture and difficult to repair can be the cause of plasma membrane disruption in many necrotic cell deaths. Alternation of biogenesis or trafficking of lysosomes can change the mode of cell death.

Increase of lysosomal volume is likely to be a downstream event in the cell death process because treatment of MCF-7 and Jurkat cells with caspase inhibitor zVAD inhibited the increase of VAC in these cells (data not shown), indicating that the lysosomal response is at least downstream of initiator caspase in these cells. However, caspase activation is not indispensable for the lysosomal response because zVAD had no effect on VAC in TNF-α-treated L929 cells (data not shown). The size of lysosomes can be altered for many different reasons. There are a number of genetic mutations that lead to the enlargement of lysosomes (2, 13, 27, 38, 43). As shown in Fig. 4A, plasma membrane disruptions were found in almost all of the TNF-α-treated *beige* fibroblasts, which had large lysosomes. It is very likely that the increased necrosis contributes to the clinical symptoms seen in this mutant. Unlike its effect in *beige* cells, deficiency of PMCA4 in L929 cells affected lyso-

or without TNF-α plus CHX. Relative values of the VAC were determined at different time points after TNF-α–CHX addition. The percent increases of the VAC are shown. (E) MCF-7 cells were treated as described for panel D and analyzed by PI exclusion plus FSC. The percentages of R1 and R2 cells are shown. (F) MCF-7 cells with or without the depletion of ATP were treated with TNF-α plus CHX in the presence or absence of forskolin (FSK; 100 μM). The viability of cells was analyzed by PI exclusion plus FSC. The percentages of R1 and R2 cells are shown. Intracellular ATP levels before and after ATP depletion were measured and are shown. Olig, oligomycin.

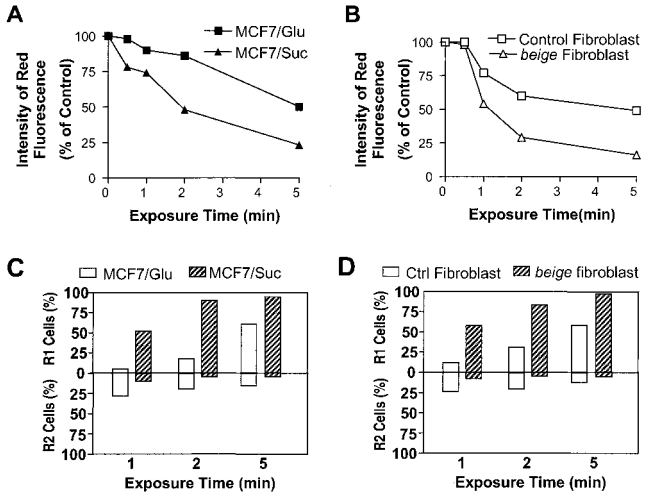

FIG. 7. Large lysosomes are easy to disrupt, and lysosomal leakage can lead to plasma membrane disruption. (A) MCF-7 cells were cultured in sucrose- or glucose-containing medium for 12 h. The cells were loaded with acridine orange for 15 min and then exposed to blue light (10×10^4 lx) for different periods of time. Lysosome leakage was determined by the decrease of red fluorescence measured by flow cytometry. (B) Fibroblasts isolated from *beige* or control (C57BL/6) mice were used to perform the same experiments as described for panel A. (C) Viability of MCF-7 cells was measured 4 h after exposure to blue light. The percentages of R1 and R2 cells are shown. (D) Viability of fibroblasts was determined as described for panel C).

some trafficking and resulted in the inhibition of the TNF-α-induced increase of lysosome size (41). The plasma membrane was better preserved in cells with mutated PMCA4 than in the corresponding wild-type cells after TNF-α treatment (Fig. 1). Changes in lysosome properties have been observed during senescence (30). We have shown here that the change of lysosomes in senescence can be determined by measuring the VAC (Fig. 4B). There was an increase of the VAC during senescence that correlated with plasma membrane disruption during cell death (Fig. 4). The increased susceptibility of senescent cells to plasma membrane disruption during cell death could contribute to the increased chronic inflammation in aged individuals. In addition to the intrinsic changes that can modify the lysosomal status in cells, the extracellular environment also can alter lysosome size. ATP depletion-mediated conversion from apoptosis to necrosis is a prototypic example of the switching between the two modes of cell death (11, 31). We found that the ATP depletion-mediated change in death modes related to lysosomal responses and that an increased lysosomal size is a cause of plasma membrane disruption (Fig. 5). In addition, culturing cells in indigestible sucrose-containing medium increased the lysosome size and resulted in the loss of plasma membrane integrity during cell death (Fig. 3). Collectively, our data demonstrated that lysosome size could be altered by either intrinsic cellular changes or extracellular environments through modifying the biogenesis and/or trafficking of the lysosomes. The condition of lysosomes in dying cells determines whether the plasma membrane integrity is maintained or lost.

There is a large body of evidence suggesting that lysosomes are involved in the cell death processes (5, 8, 25, 32, 39, 40). We have previously shown that an increase in the total volume of lysosomes is a common event in cell death induced by diverse stimuli (41). We have also shown that the disintegration of lysosomes in TNF-α-treated L929 cells occurs prior to plasma membrane disruption, suggesting that lysosome rupture is responsible for the necrosis phenotype in L929 cell death (41). A similar observation of the disintegration of lysosomes prior to membrane rupture in other cell death systems was reported (59). An increase in the total volume of lysosomes was believed to represent an increase of lysosome activity (34). This event may be required for the self-digestion of cellular components during programmed cell death. Findings concerning autophagic cell death, a type of death described almost 40 years ago, also support the role of lysosomal biogenesis and trafficking in cell death (48). As reviewed by Bursch and Lockshin et al., autophagic cell death is characterized by visible autophagic vacuoles (6, 35). Unlike what is found in apoptosis, degradation of cytoplasmic components precedes nuclear collapse in autophagic cell death. There are some similarities between the cell death that we studied and autophagic cell death. The increase of acidic vacuoles in TNF-α-treated cells is similar to that in cells in the later stages of autophagic death, in which autophagic bodies fuse with lysosomes. However, TNF-α-induced acidic vacuoles are unlikely to be derived from autophagic vacuoles because 3-methyladenine, an inhibitor of the sequestration step in the formation of autophagic vacuoles, does not affect the TNF-α-induced increase of acidic vacuoles and cell death (data not shown). Since an autophagosome docks and fuses with a lysosome and breaks down within the lysosome for degradation, the biogenesis and trafficking of lysosomes should be induced in autophagic cell death too. It is well established that most organelles of a dying cell manifest subtle biochemical alterations, in particular proteolysis (14). Lysosomes most likely participate in the self-digestion of many intracellular components during cell death, either through autophagy or other mechanisms. The increased biogenesis and trafficking of lysosomes are a part of the cell death program. An accidental rupture of lysosomes can occur in this part of the death program and cause necrosis. This may explain why necrosis can occur in the same cell death system and why secondary necrosis is often associated with apoptosis. The rupture of lysosomes is not an accident in cells such as L929 but rather is a part of the necrosis process. It is probable that the TNF-α-induced biogenesis or trafficking of lysosomes in these cells is imbalanced, which would result in oversized lysosomes and subsequent lysosomal disruption.

There are reports suggesting that the release of lysosomal enzymes can initiate apoptosis (17, 44, 45). A prevalent assumption is that reparable damage of lysosomes can initiate apoptosis and that a sudden massive destruction of lysosomes will then lead to cell lysis (necrosis) (14). Lysosomal enzymes cathepsin B and D were reported to be required for cell death induced by TNF-α and other death stimuli (8, 49). More recently, lysosomal protease cathepsin B was found to be involved in amplifying the death signaling in TNF-α-treated hepatocytes, suggesting that release of the contents of lysosomes can be an active process rather than a solely passive result of accidental rupture (17). It is unknown whether lysosomal rupture (transient or permanent) is a regulatory mechanism for cathepsin B and D release from lysosomes or if a special transporting mechanism is involved in translocating

cathepsin B and D into cytosol. Since there is no doubt that lysosomal enzymes can cause cell lysis, the plasma membrane can be disrupted if a sufficient amount of these enzymes is released from lysosomes.

Plasma membrane disruption should be the key characteristic that distinguishes necrosis from apoptosis in terms of biological consequences. The level of lysosomal rupture determines whether the plasma membrane remains intact or ruptures in many, if not all, cell death processes. The lysosomal disruption in necrotic cell death could be as important as nuclear fragmentation in apoptosis. Intrinsic and extrinsic factors under physiological or pathological conditions can alter the size and other properties of lysosomes and increase or decrease their susceptibility to rupture. The cells that have big lysosomes tend to lose their plasma membrane when death is induced. The cells that have abnormal inductions of lysosomal volume during death also have a greater chance for plasma membrane disruption. Since the size of the lysosomal volume in cells at rest or after exposure to death stimuli determines whether the integrity of the plasma membrane can be maintained, attention should be given to lysosomal biogenesis and/or trafficking in order to understand how necrosis occurs in physiological or pathological conditions.

ACKNOWLEDGMENTS

We thank J. C. Reed (Burnham Institute, La Jolla, Calif.) for helpful comments and T. Thompson for excellent secretarial assistance.

This work was supported by U.S. Public Health Service grant no.AI41637 from the National Institute of Allergy and Infectious Diseases and California Cancer Research Program subcontract no. 99-00521V-10121.

REFERENCES

1. **Andrews, N. W.** 2000. Regulated secretion of conventional lysosomes. Trends. Cell Biol. **10:**316–321.
2. **Barbosa, M. D., Q. A. Nguyen, V. T. Tchernev, J. A. Ashley, J. C. Detter, S. M. Blaydes, S. J. Brandt, D. Chotai, C. Hodgman, R. C. Solari, M. Lovett, and S. F. Kingsmore.** 1996. Identification of the homologous beige and Chediak-Higashi syndrome genes. Nature **382:**262–265.
3. **Beyaert, R., and W. Fiers.** 1994. Molecular mechanisms of tumor necrosis factor-induced cytotoxicity. What we do understand and what we do not. FEBS Lett. **340:**9–16.
4. **Brunk, U. T., H. Dalen, K. Roberg, and H. B. Hellquist.** 1997. Photo-oxidative disruption of lysosomal membranes causes apoptosis of cultured human fibroblasts. Free Radic. Biol. Med. **23:**616–626.
5. **Brunk, U. T., and I. Svensson.** 1999. Oxidative stress, growth factor starvation and Fas activation may all cause apoptosis through lysosomal leak. Redox Rep. **4:**3–11.
6. **Bursch, W.** 2001. The autophagosomal-lysosomal compartment in programmed cell death. Cell Death Differ. **8:**569–581.
7. **Cohn, Z. A., and B. A. Ehrenreich.** 1969. The uptake, storage, and intracellular hydrolysis of carbohydrates by macrophages. J. Exp. Med. **129:**201–225.
8. **Deiss, L. P., H. Galinka, H. Berissi, O. Cohen, and A. Kimchi.** 1996. Cathepsin D protease mediates programmed cell death induced by interferon-gamma, Fas/APO-1 and TNF-alpha. EMBO J. **15:**3861–3870.
9. **Doi, T., N. Motoyama, A. Tokunaga, and T. Watanabe.** 1999. Death signals from the B cell antigen receptor target mitochondria, activating necrotic and apoptotic death cascades in a murine B cell line, WEHI-231. Int. Immunol. **11:**933–941.
10. **Drenou, B., V. Blancheteau, D. H. Burgess, R. Fauchet, D. J. Charron, and N. A. Mooney.** 1999. A caspase-independent pathway of MHC class II antigen-mediated apoptosis of human B lymphocytes. J. Immunol. **163:**4115–4124.
11. **Eguchi, Y., S. Shimizu, and Y. Tsujimoto.** 1997. Intracellular ATP levels determine cell death fate by apoptosis or necrosis. Cancer Res. **57:**1835–1840.
12. **Fady, C., A. Gardner, F. Jacoby, K. Briskin, Y. Tu, I. Schmid, and A. Lichtenstein.** 1995. Atypical apoptotic cell death induced in L929 targets by exposure to tumor necrosis factor. J. Interferon Cytokine Res. **15:**71–80.
13. **Feng, L., A. B. Seymour, S. Jiang, A. To, A. A. Peden, E. K. Novak, L. Zhen, M. E. Rusiniak, E. M. Eicher, M. S. Robinson, M. B. Gorin, and R. T. Swank.** 1999. The beta3A subunit gene (Ap3b1) of the AP-3 adaptor complex is altered in the mouse hypopigmentation mutant pearl, a model for Hermansky-Pudlak syndrome and night blindness. Hum. Mol. Genet. **8:**323–330.
14. **Ferri, K. F., and G. Kroemer.** 2001. Organelle-specific initiation of cell death pathways. Nat. Cell Biol. **3:**E255–E263.
15. **Fiers, W., R. Beyaert, W. Declercq, and P. Vandenabeele.** 1999. More than one way to die: apoptosis, necrosis and reactive oxygen damage. Oncogene **18:**7719–7730.
16. **Goossens, V., J. Grooten, K. De Vos, and W. Fiers.** 1995. Direct evidence for tumor necrosis factor-induced mitochondrial reactive oxygen intermediates and their involvement in cytotoxicity. Proc. Natl. Acad. Sci. USA **92:**8115–8119.
17. **Guicciardi, M. E., J. Deussing, H. Miyoshi, S. F. Bronk, P. A. Svingen, C. Peters, S. H. Kaufmann, and G. J. Gores.** 2000. Cathepsin B contributes to TNF-alpha-mediated hepatocyte apoptosis by promoting mitochondrial release of cytochrome c. J. Clin. Investig. **106:**1127–1137.
18. **Ha, H. C., and S. H. Snyder.** 1999. Poly(ADP-ribose) polymerase is a mediator of necrotic cell death by ATP depletion. Proc. Natl. Acad. Sci. USA **96:**13978–13982.
19. **Herceg, Z., and Z. Q. Wang.** 1999. Failure of poly(ADP-ribose) polymerase cleavage by caspases leads to induction of necrosis and enhanced apoptosis. Mol. Cell. Biol. **19:**5124–5133.
20. **Hildeman, D. A., T. Mitchell, T. K. Teague, P. Henson, B. J. Day, J. Kappler, and P. C. Marrack.** 1999. Reactive oxygen species regulate activation-induced T cell apoptosis. Immunity **10:**735–744.
21. **Holler, N., R. Zaru, O. Micheau, M. Thome, A. Attinger, S. Valitutti, J. L. Bodmer, P. Schneider, B. Seed, and J. Tschopp.** 2000. Fas triggers an alternative, caspase-8-independent cell death pathway using the kinase RIP as effector molecule. Nat. Immunol. **1:**489–495.
22. **Humphreys, D. T., and M. R. Wilson.** 1999. Modes of L929 cell death induced by TNF-alpha and other cytotoxic agents. Cytokine **11:**773–782.
23. **Jacotot, E., P. Costantini, E. Laboureau, N. Zamzami, S. A. Susin, and G. Kroemer.** 1999. Mitochondrial membrane permeabilization during the apoptotic process. Ann. N. Y. Acad. Sci. **887:**18–30.
24. **Jahraus, A., B. Storrie, G. Griffiths, and M. Desjardins.** 1994. Evidence for retrograde traffic between terminal lysosomes and the prelysosomal/late endosome compartment. J. Cell Sci. **107:**145–157.
25. **Jia, L., R. R. Dourmashkin, P. D. Allen, A. B. Gray, A. C. Newland, and S. M. Kelsey.** 1997. Inhibition of autophagy abrogates tumour necrosis factor alpha induced apoptosis in human T-lymphoblastic leukaemic cells. Br. J. Haematol. **98:**673–685.
26. **Kane, D. J., T. A. Sarafian, R. Anton, H. Hahn, E. B. Gralla, J. S. Valentine, T. Ord, and D. E. Bredesen.** 1993. Bcl-2 inhibition of neural death: decreased generation of reactive oxygen species. Science **262:**1274–1277.
27. **Kantheti, P., X. Qiao, M. E. Diaz, A. A. Peden, G. E. Meyer, S. L. Carskadon, D. Kapfhamer, D. Sufalko, M. S. Robinson, J. L. Noebels, and M. Burmeister.** 1998. Mutation in AP-3 delta in the mocha mouse links endosomal transport to storage deficiency in platelets, melanosomes, and synaptic vesicles. Neuron **21:**111–122.
28. **Kawahara, A., Y. Ohsawa, H. Matsumura, Y. Uchiyama, and S. Nagata.** 1998. Caspase-independent cell killing by Fas-associated protein with death domain. J. Cell Biol. **143:**1353–1360.
29. **Kroemer, G., B. Dallaporta, and M. Resche-Rigon.** 1998. The mitochondrial death/life regulator in apoptosis and necrosis. Annu. Rev. Physiol. **60:**619–642.
30. **Kurz, D. J., S. Decary, Y. Hong, and J. D. Erusalimsky.** 2000. Senescence-associated (beta)-galactosidase reflects an increase in lysosomal mass during replicative ageing of human endothelial cells. J. Cell Sci. **113:**3613–3622.
31. **Leist, M., B. Single, A. F. Castoldi, S. Kuhnle, and P. Nicotera.** 1997. Intracellular adenosine triphosphate (ATP) concentration: a switch in the decision between apoptosis and necrosis. J. Exp. Med. **185:**1481–1486.
32. **Liddil, J. D., R. T. Dorr, and P. Scuderi.** 1989. Association of lysosomal activity with sensitivity and resistance to tumor necrosis factor in murine L929 cells. Cancer Res. **49:**2722–2728.
33. **Liu, Z. G., and J. Han.** 2001. Cellular responses to tumor necrosis factor. Curr. Issues Mol. Biol. **3:**79–90.
34. **Lloyd, J. B.** 1996. The taxonomy of lysosomes and related structures. Subcell. Biochem. **27:**1–13.
35. **Lockshin, R. A., B. Osborne, and Z. Zakeri.** 2000. Cell death in the third millennium. Cell Death Differ. **7:**2–7.
36. **Los, M., M. Mozoluk, D. Ferrari, A. Stepczynska, C. Stroh, A. Renz, Z. Herceg, Z. Q. Wang, and K. Schulze-Osthoff.** 2002. Activation and caspase-mediated inhibition of PARP: a molecular switch between fibroblast necrosis and apoptosis in death receptor signaling. Mol. Biol. Cell **13:**978–988.
37. **Mateo, V., L. Lagneaux, D. Bron, G. Biron, M. Armant, G. Delespesse, and M. Sarfati.** 1999. CD47 ligation induces caspase-independent cell death in chronic lymphocytic leukemia. Nat. Med. **5:**1277–1284.
38. **Nagle, D. L., M. A. Karim, E. A. Woolf, L. Holmgren, P. Bork, D. J. Misumi, S. H. McGrail, B. J. Dussault, C. M. Perou, R. E. Boissy, G. M. Duyk, R. A. Spritz, and K. J. Moore.** 1996. Identification and mutation analysis of the complete gene for Chediak-Higashi syndrome. Nat. Genet. **14:**307–311.

39. **Ohsawa, Y., K. Isahara, S. Kanamori, M. Shibata, S. Kametaka, T. Gotow, T. Watanabe, E. Kominami, and Y. Uchiyama.** 1998. An ultrastructural and immunohistochemical study of PC12 cells during apoptosis induced by serum deprivation with special reference to autophagy and lysosomal cathepsins. Arch. Histol. Cytol. **61:**395–403.
40. **Ollinger, K., and U. T. Brunk.** 1995. Cellular injury induced by oxidative stress is mediated through lysosomal damage. Free Radic. Biol. Med. **19:** 565–574.
41. **Ono, K., X. Wang, and J. Han.** 2001. Resistance to tumor necrosis factor-induced cell death mediated by PMCA4 deficiency. Mol. Cell. Biol. **21:**8276–8288.
42. **Penninger, J. M., and G. Kroemer.** 1998. Molecular and cellular mechanisms of T lymphocyte apoptosis. Adv. Immunol. **68:**51–144.
43. **Perou, C. M., J. D. Leslie, W. Green, L. Li, D. M. Ward, and J. Kaplan.** 1997. The Beige/Chediak-Higashi syndrome gene encodes a widely expressed cytosolic protein. J. Biol. Chem. **272:**29790–29794.
44. **Roberg, K., U. Johansson, and K. Ollinger.** 1999. Lysosomal release of cathepsin D precedes relocation of cytochrome c and loss of mitochondrial transmembrane potential during apoptosis induced by oxidative stress. Free Radic. Biol. Med. **27:**1228–1237.
45. **Roberg, K., and K. Ollinger.** 1998. Oxidative stress causes relocation of the lysosomal enzyme cathepsin D with ensuing apoptosis in neonatal rat cardiomyocytes. Am. J. Pathol. **152:**1151–1156.
46. **Rodriguez, A., I. Martinez, A. Chung, C. H. Berlot, and N. W. Andrews.** 1999. cAMP regulates Ca^{2+}-dependent exocytosis of lysosomes and lysosome-mediated cell invasion by trypanosomes. J. Biol. Chem. **274:**16754–16759.
47. **Rodriguez, A., P. Webster, J. Ortego, and N. W. Andrews.** 1997. Lysosomes behave as Ca^{2+}-regulated exocytic vesicles in fibroblasts and epithelial cells. J. Cell Biol. **137:**93–104.
48. **Schweichel, J. U., and H. J. Merker.** 1973. The morphology of various types of cell death in prenatal tissues. Teratology **7:**253–266.
49. **Shibata, M., S. Kanamori, K. Isahara, Y. Ohsawa, A. Konishi, S. Kametaka, T. Watanabe, S. Ebisu, K. Ishido, E. Kominami, and Y. Uchiyama.** 1998. Participation of cathepsins B and D in apoptosis of PC12 cells following serum deprivation. Biochem. Biophys. Res. Commun. **251:**199–203.
50. **Shimizu, S., Y. Eguchi, H. Kosaka, W. Kamiike, H. Matsuda, and Y. Tsujimoto.** 1995. Prevention of hypoxia-induced cell death by Bcl-2 and Bcl-xL. Nature **374:**811–813.
51. **Swanson, J., B. Yirinec, E. Burke, A. Bushnell, and S. C. Silverstein.** 1986. Effect of alterations in the size of the vacuolar compartment on pinocytosis in J774.2 macrophages. J. Cell. Physiol. **128:**195–201.
52. **Tafani, M., T. G. Schneider, J. G. Pastorino, and J. L. Farber.** 2000. Cytochrome c-dependent activation of caspase-3 by tumor necrosis factor requires induction of the mitochondrial permeability transition. Am. J. Pathol. **156:**2111–2121.
53. **Tewari, M., and V. M. Dixit.** 1995. Fas- and tumor necrosis factor-induced apoptosis is inhibited by the poxvirus crmA gene product. J. Biol. Chem. **270:**3255–3260.
54. **Vandevoorde, V., G. Haegeman, and W. Fiers.** 1997. Induced expression of trimerized intracellular domains of the human tumor necrosis factor (TNF) p55 receptor elicits TNF effects. J. Cell Biol. **137:**1627–1638.
55. **Vercammen, D., R. Beyaert, G. Denecker, V. Goossens, G. Van Loo, W. Declercq, J. Grooten, W. Fiers, and P. Vandenabeele.** 1998. Inhibition of caspases increases the sensitivity of L929 cells to necrosis mediated by tumor necrosis factor. J. Exp. Med. **187:**1477–1485.
56. **Wang, X., and J. Han.** 2000. Elucidating tumor necrosis factor signaling pathway using a functional gene identification approach. Immunol. Res. **21:**1–7.
57. **Wang, X., K. Ono, S. O. Kim, V. Kravchenko, S. C. Lin, and J. Han.** 2001. Metaxin is required for tumor necrosis factor-induced cell death. EMBO Rep. **2:**628–633.
58. **Xiang, J., D. T. Chao, and S. J. Korsmeyer.** 1996. BAX-induced cell death may not require interleukin 1β-converting enzyme-like proteases. Proc. Natl. Acad. Sci. USA **93:**14559–14563.
59. **Zahrebelski, G., A. L. Nieminen, K. al-Ghoul, T. Qian, B. Herman, and J. J. Lemasters.** 1995. Progression of subcellular changes during chemical hypoxia to cultured rat hepatocytes: a laser scanning confocal microscopic study. Hepatology **21:**1361–1372.